J Comput Aided Mol Des (2010) 24:77–87
DOI 10.1007/s10822-009-9315-y

Characterization of dipeptidylcarboxypeptidase of *Leishmania donovani*: a molecular model for structure based design of antileishmanials

Mirza Saqib Baig · Ashutosh Kumar · Mohammad Imran Siddiqi · Neena Goyal

Received: 1 July 2009 / Accepted: 6 December 2009 / Published online: 29 December 2009

Abstract *Leishmania donovani* dipeptidylcarboxypeptidsae (LdDCP), an angiotensin converting enzyme (ACE) related metallopeptidase has been identified and characterized as a putative drug target for antileishmanial chemotherapy. The kinetic parameters for LdDCP with substrate, Hip-His-Leu were determined as, Km, 4 mM and Vmax, 1.173 μmole/ml/min. Inhibition studies revealed that known ACE inhibitors (captopril and bradykinin potentiating peptide; BPP1) were weak inhibitors for LdDCP as compared to human testicular ACE (htACE) with Ki values of 35.8 nM and 3.9 μM, respectively. Three dimensional model of LdDCP was generated based on crystal structure of *Escherichia coli* DCP (EcDCP) by means of comparative modeling and assessed using PROSAII, PROCHECK and WHATIF. Captopril docking with htACE, LdDCP and EcDCP and analysis of molecular electrostatic potentials (MEP) suggested that the active site domain of three enzymes has several minor but potentially important structural differences. These differences could be exploited for designing selective inhibitor of LdDCP thereby antileishmanial compounds either by denovo drug design or virtual screening of small molecule databases.

Keywords Dipeptidylcarboxypeptidase · *Leishmania donovani* · Enzyme kinetics · Homology modeling · Docking · Molecular electrostatic potentials

Introduction

Protozoan parasites of the genus *Leishmania* cause a wide spectrum of diseases (visceral, cutaneous and mucosal) in humans collectively referred to as leishmaniasis [1]. The disease is prevalent in 88 countries with approximately 400,000 new cases per year [2]. The traditionally exotic disease leishmaniasis is becoming of greater interest for two main reasons, the international travel and importance of *Leishmania* as opportunists in AIDS patients (http://www.who.int/emc/diseases/leish/leishdisl.html). It is an emerging tropical disease in United States with more than 500 parasitological confirmed cases (http://www.cdc.gov/ncidod/diseases/submenus/sub_leishmania.htm). The parasite leads digenetic life cycle with an extracellular promastigote stage in sand fly vector and an intracellular amastigote stage occurring within mammalian macrophages [3]. It is the amastigote form, which is responsible for pathogenicity due to its ability to encounter the hostile environment of the phagolysosome. Vaccines against leishmaniasis are still under development and therapies are inadequate with sever toxic side effects and high cost. Further, a large scale increase of clinical resistance to the drug of first choice, pentavalent antimonials has been reported [4, 5]. Consequently, need for novel chemotherapeutic approaches in the fight against Leishmaniasis are

Mirza Saqib Baig and Ashutosh Kumar have contributed equally to this work.

Electronic supplementary material The online version of this article (doi:10.1007/s10822-009-9315-y) contains supplementary material, which is available to authorized users.

A. Kumar · M. I. Siddiqi
Division of Molecular and Structural Biology, Central Drug Research Institute, Lucknow 226001, India

M. S. Baig · N. Goyal (✉)
Division of Biochemistry, Central Drug Research Institute, Lucknow 226001, India
e-mail: neenacdri@yahoo.com

imperative. Current hope lies in research program oriented towards identification and characterization of key process essential for parasite growth, survival in mammalian host and transmission by its insect vector that can serve as drug targets. One such putative target is *L. donovani* dipeptidylcarboxypeptidase (LdDCP), an angiotensin converting enzyme (ACE) related metallopeptidase. It has been identified for the first time in any kinetoplast protozoan and found upregulated in amastigotes, the mammalian stage of the parasite [6]. LdDCP belongs to M3 family of mono zinc peptidases and cleaves Hip-His-Leu, a substrate for ACE to release hippuric acid. Captopril, a known ACE inhibitor, was able to inhibit both LdDCP enzyme activity and in vitro parasite multiplication. These observations clearly indicated the therapeutic potential of parasite enzyme inhibition. Further, LdDCP was lesser sensitive to captopril as compared to mammalian ACE, suggesting that selective inhibitors of LdDCP could serve as potential leads for *Leishmania* chemotherapy. With known crystal structure of an enzyme, the drug design process is significantly facilitated. However, one is frequently faced the situation where a ligand has to be designed for a target protein for which no experimentally determined structure is available. In such cases, comparative protein structure modeling can be employed [7]. The comparative approach to protein structure prediction is based on the fact that structure is more conserved than sequences during evolution [8]. Therefore, proteins that share even low sequence similarity, many times also have similar function [9].

In the present study, we describe 3D structural model for LdDCP using the X-ray crystal structure of DCP from *E. coli* [10] with an aim to reveal the differences in binding modes of captopril with LdDCP, EcDCP and ACE that can be exploited to understand the ligand binding interaction and may also in the development of anti-leishmanial compounds.

Methodology

Enzyme assay and inhibition studies

Recombinant leishmanial DCP was expressed in *E. coli* BL21 (DE3) pLys expression host and purified to homogeneity as described earlier [6] Purity of the recombinant enzyme was checked on SDS-PAGE [11]. Enzyme activity was measured according to the method of Cushman and Cheung, using *N*-benzoyl-L-glycyl-L-histidyl-L-leucine (HHL), a routine substrate used for angiotensin converting enzyme (ACE) [12]. DCP releases hippuric acid from HHL, which absorbs at 228 nm. One unit of enzyme activity is defined, as the amount of enzyme required to release 1 μmole of hippuric acid per minute at 37 °C taking extension coefficient of hippuric acid, 9.8 $mM^{-1}cm^{-1}$. Protein concentration was determined by Bradford method using bovine serum albumin as standard [13]. To determine Km and Vmax of LdDCP, enzyme activity was assayed at varying concentrations (0.25–10 mM) of the substrate. The kinetic data was analyzed by linear regression fit to Michaelis-Menten plot. Effect of ACE inhibitors namely captopril and bradykinin potentiating peptide (BPP1; pGlu-Trp-Pro-Arg-Pro-Gln-Ile-Pro-Pro) were studied on the activity of LdDCP. Different concentrations of inhibitor were incubated with the enzyme for 5 min prior to the addition of the substrate.

Circular dichroism measurements

CD measurements were carried out on a Jasco spectropolarimeter Model J-810 (Jasco International Co., Ltd, Tokyo, Japan) fitted with a thermostatically controlled cell holder having an accuracy of ±0.1 °C. Calibration of the spectropolarimeter was performed with ammonium (+)-10-camphorsulfonic acid. Results were expressed as relative ellipticity [θ], which is defined as [θ] = 100 x θobs/(lc), where θobs is the observed ellipticity in degrees, c is the concentration in moles of residue per liter and l is the length of the light path in centimeters. The CD spectrum was measured at an enzyme concentration of 3.0 μM with a 1 mm cell at 25 °C. The values obtained were normalized by subtracting the baseline recorded for the buffer. The buffer used for spectroscopy was 40 mM sodium phosphate (pH 7.4), 100 mM NaCl. The percentage of secondary structure was determined by K2d program (www.embl-heidelberg.de/~andrade/k2d.html).

Sequence alignment

Sequence alignment between *L. donovani* DCP and *E. coli* DCP was generated using CLUSTAL W provided in the homology module of InsightII (Insight II Program, Accelrys Inc., San Diego, CA, 2001).

Homology modeling

For modeling of the LdDCP, we used restrained-based modeling, implemented in the MODELLER program interfaced with homology module of InsightII 2000.1 [14]. This program is an automated approach to comparative modeling by satisfaction of spatial restraints. Recently deduced crystal structure of EcDCP (PDB access code: 1Y79) was used as a template. Primary sequence alignment established that LdDCP and EcDCP share 45.3% identity (similarity 67.1%) with one conserved zinc binding signature sequence His-Glu-X-X-His. For such a sequence

identity, it has been shown that homology modeling yields a structure that is accurate enough for use in computational studies [15–17]. The homology model obtained by the MODELLER was further refined by energy minimization, first by 200 steps of steepest descent and then by 1,000 steps by conjugate gradient method using CVFF force field using DISCOVER_3 module of InsightII 2000.1. The refined LdDCP model was subjected to a series of three tests. Backbone conformation was evaluated by the inspection of Psi/Phi Ramachandran plot obtained from PROCHECK analysis [18]. The PROSA test [19] was applied to check for energy criteria in comparison with the potential of mean force derived from a large set of known protein structure. Packing quality of refined structure was investigated by the calculation of WHATIF [19, 20]. Further, the root mean square deviation (RMSD) between the main chain atom of model and template was calculated for the reliability of the model.

Molecular docking

Three-dimensional structure of captopril was constructed using the SYBYL7.1 suite of programs (TRIPOS Inc. 1699, South Hanley Road, St. Louis, Mo 63144, USA) running under Irix 6.5. Captopril was docked into the active sites of human angiotensin converting enzyme (ACE), EcDCP and LdDCP using the FlexX program interfaced with Sybyl 7.1(FlexX, version 1.13.5; Saint Augustin, Germany, BioSolveIT GmbH). The active site regions for the comparative FlexX docking simulations of captopril were specified on the basis of previously reported structural information of human testicular ACE [21] complexed with captopril. The proposed interaction modes of the captopril with the binding site were determined with the highest scored conformation (best-fit ligand) with C-Score value of 5 among 30 conformational and binding modes generated. According to the FlexX scoring this conformation was represented by the structure with the most favorable binding free energy. The binding mode conformations derived from FlexX docking, were rechecked using second molecular docking softeware, LigandFit, interfaced with Cerius2.49 molecular modeling package (Cerius2, Version 4.10; Accelrys, Inc. San Diego, CA, USA, 2005) using default parameters. The zinc parameters for the docking simulations were imported from the work of Stote and Karplus comprising of charge = 2.0, ionic radius = 1.1 Å and well depth of 0.35 kcal/mol.

The selectivity of captopril binding with three functionally similar enzymes was further evaluated by calculating MM/PBSA residues interaction energy of bound conformation of captopril derived from docking using Discovery studio package (Discovery Studio, Version 2.5; Accelrys, Inc. San Diego, CA, USA, 2009).

Molecular electrostatic potential

All molecular electrostatic potential calculations were carried out using the GRASP program [22] and the molecular electrostatic potential were visualized using UCSF Chimera [23, 24]. The color ramp for electrostatic potential ranges from red (most negative) to blue (most positive).

Results and discussion

Kinetic properties of LdDCP

Peptidases of parasitic protozoa are currently the subject of intensive investigation in the hope of identifying novel drug targets and vaccine candidates. In *Leishmania,* very few have received considerable attention that includes lysosomal cysteine peptidases [25], membrane bound zinc metalloprotease (GP63) [26], serine type oligopeptidase B [27] and leucyl aminopeptidase [28]. Recently, we identified an ACE related dipeptidyl carboxypeptidase in *L. donovani* which is up regulated in mammalian stage of parasite [6]. This is the first demonstration of such an enzyme in any protozoan parasite. Dipeptidylcarboxypeptidase (DCP)/peptidyl dipeptidase, first described in *E. coli* cleaves dipeptides of the C-termini of various peptides and proteins, the smallest substrate being N-blocked tripeptides and unblocked tetra peptides [29]. In the mammalian system, the same function is performed by peptidyl dipeptidase A, also known as angiotensin converting enzyme (ACE) [30]. LdDCP belongs to the zinc metallopeptidase family and cleaves N-benzoyal-L-glycyl-L- histidyl-L-leucine (HHL), a substrate for ACE as well as bacterial DCP to release hippuric acid [6]. *Leishmanial* DCP followed Michaelis-Menten kinetics for the substrate HHL and the kinetic parameters were determined using the Lineweaver–Burk plot (Fig. 1). The Km and Vmax for Hip-His-Leu were calculated to be 4 mM and 1.173 μmole/ml/min, respectively. Km value of LdDCP enzyme is approximately 2.58 fold higher than the Km of *E. coli* K-12 DCP and 2.35 fold than human testicular ACE [31, 32]. Higher Km suggests lower affinity of HHL towards active site of LdDCP as compared to EcDCP and human testicular ACE. Although, LdDCP was shown to be inhibited by a known ACE inhibitor, captopril but, the enzyme was much less sensitive than mammalian ACE [6]. Figure 2a depicts the Dixon plot for inhibition of LdDCP at various concentrations of captopril. Analysis revealed a competitive mode of inhibition and reversible inhibition constant (Ki) was determined to be 35.8 nM. Interestingly, this value is 2.56 fold higher than value reported for human testicular ACE [33]. *E. coli* DCP exhibited a comparable exquisite sensitivity to captopril as human ACE [34]. Further, BPP1, another ACE inhibitor

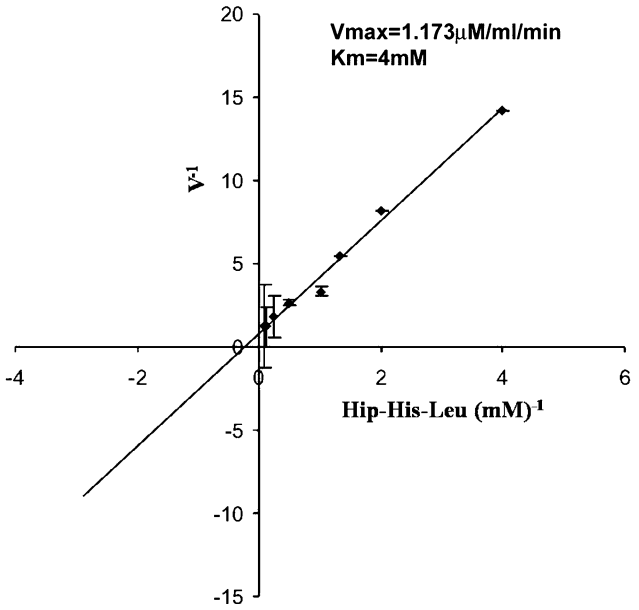

Fig. 1 Determination of Km and Vmax of LdDCP by double reciprocal (Lineweaver–Burk) plot at different concentration of substrate Hip-His-Leu. LdDCP activity was estimated by quantifying hippuric acid generation and expressed as μmoles/ml/min

also inhibits hydrolysis of HHL by LdDCP in competitive manner with a Ki value of 3.9 μM (Fig. 2b), which is several thousand folds higher than value reported for C-domain of human testicular ACE [35]. It has been shown that, cleavage of angiotensinI in vivo could be controlled solely by C-domain of human ACE [35]. The data clearly demonstrate that the two enzymes i.e. LdDCP and ACE significantly differ in their kinetic properties, which is in accordance to very low sequence homology (20.793%) between two enzymes [6]. The functional homology may be due to high of conservation in active site residues specially zinc binding residues but there may be considerable sequence variation in neighboring active site residues which is responsible for structural differences in shape and conformation of their active sites leading to catalytic variation. It would therefore be interesting to study the extent of variation and its implications in the design of effective inhibitor which can target specifically to LdDCP enzyme.

Homology model of LdDCP

The modeling procedure begins with an alignment of the sequence to be modeled (target) with related known three-dimensional structures (templates). This alignment is usually the input to the program. The output is a three-dimensional model for the target sequence containing all main-chain and side-chain non-hydrogen atoms. While choosing the template structure for the comparative modeling of LdDCP, various aspects that affect the quality of homology model such as overall sequence identity, extent of binding site conservation, size and location of insertions and deletions, and resolution were actively considered. Primary sequence alignment showed that LdDCP and EcDCP share 45.3% identity (similarity 67.1%) with one conserved zinc binding signature sequence His-Glu-X-X-His. Moreover, the amino acid composition of two enzymes was comparable: the total numbers of positively and negatively charged residues were 94 and 79 for LdDCP and 86 and 67 for EcDCP. Other properties like isoelectric points (5.74 and 5.49), instability index (II) (39.87 and 39.25), aliphatic index (79.93 and 83.50) and grand average of hydropathicity (GRAVY)

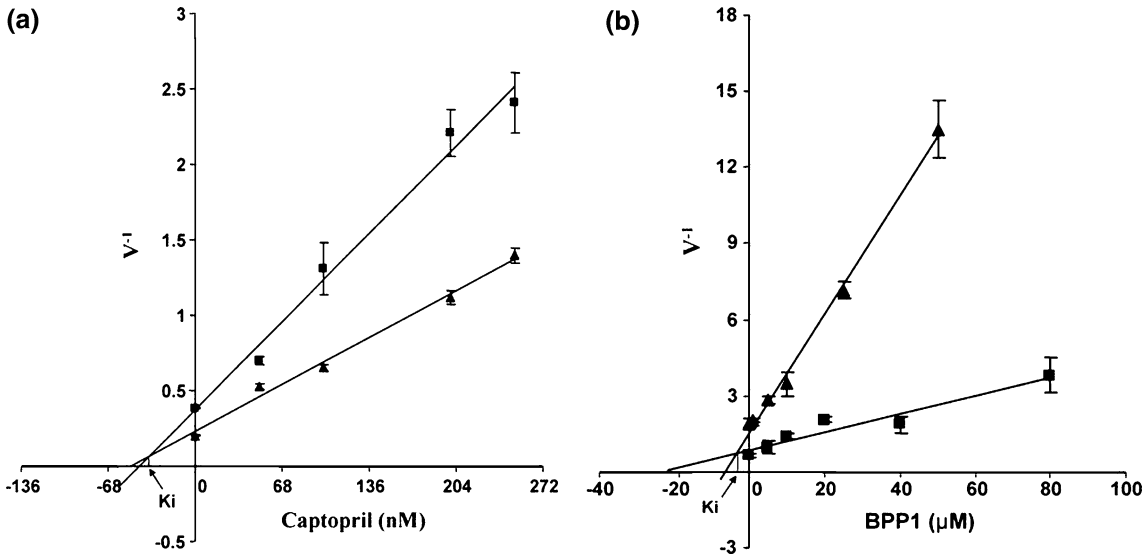

Fig. 2 **a** Plot of reciprocal of velocity as function of concentration of captopril (50−250 nM) with two (*Black square* 2 mM and *Black up pointing triangle* 4 mM) substrate concentration. **b** Plot of reciprocal of velocity as function of concentration of BPP1 (5-100 μM) with two (*Black square* 3 mM and *Black up pointing triangle* 1 mM) substrate concentration

(−0.393 and −0.334) for LdDCP and EcDCP, respectively, were also comparable. These observations suggest that EcDCP offers good choice as template for 3D modeling of LdDCP. Therefore, recently deduced crystal structure of EcDCP (PDB access code: 1Y79) was used as template. The final alignment of LdDCP (accession no. AY665610) and EcDCP, (accession no. P24171) with secondary structural elements of EcDCP is shown in Fig. 3. Like EcDCP crystal structure, the LdDCP homology model is a monomer and exhibits two separate sub domains: domain-I and domain-II (Fig. 4). LdDCP model is predominantly 57% α -helical and 6% β -secondary in nature, which is in accordance to secondary structure determined by circular dichroism spectroscopic measurements (Fig.5). The structure was primarily

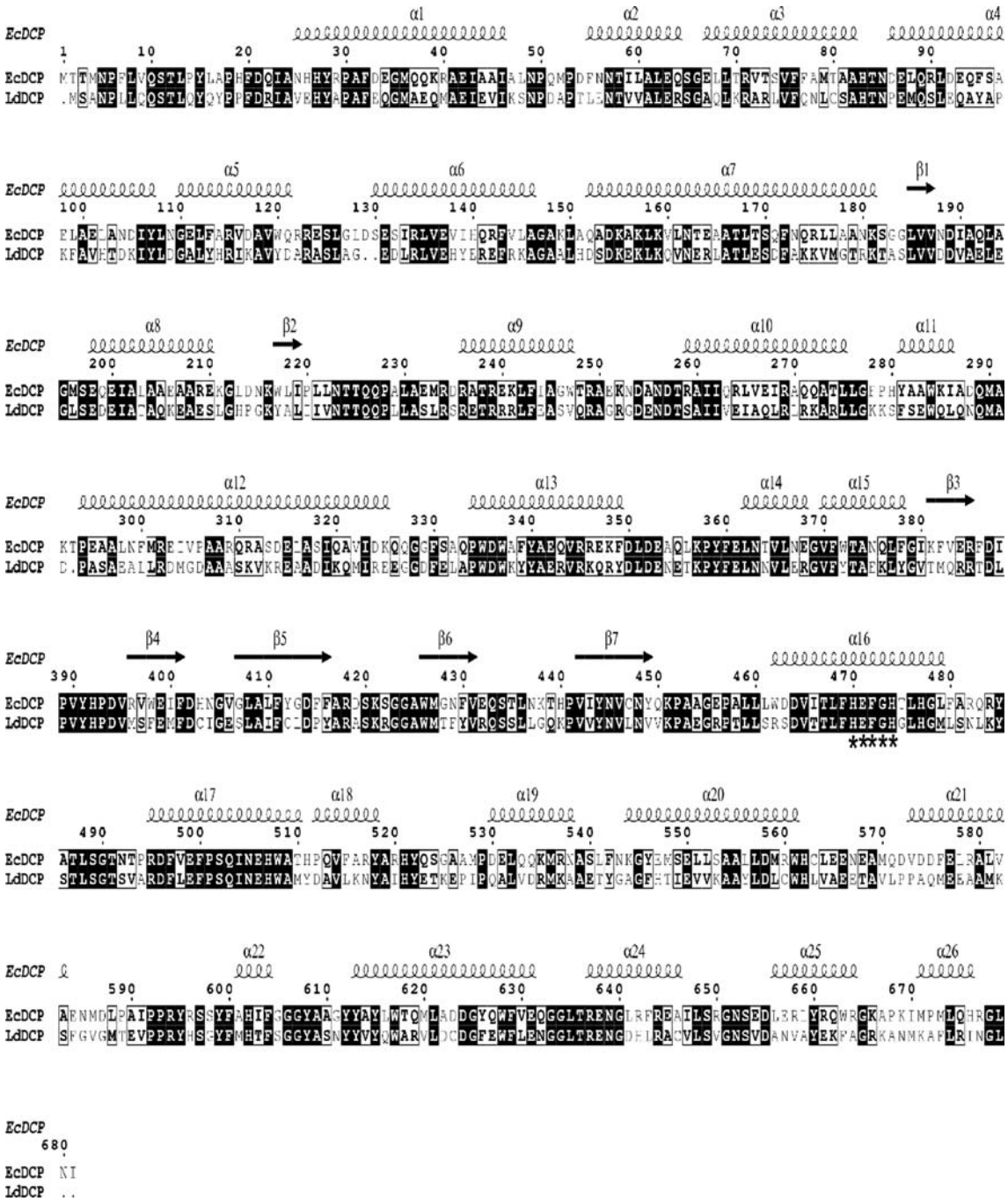

Fig. 3 Sequence alignment between LdDCP (accession no. AAV80217), and EcDCP (accession no. P24171) sequence produced by Clustal W. Alignment length: conserved regions are represented by black boxes. The secondary structure of EcDCP is demonstrated with arrows for β-sheet and spiral for α-helices. Zinc binding motif is represented by asterisk

Fig. 4 Proposed 3-D homology model of LdDCP with subdomain I and II displayed in *red* and *deep yellow color*, respectively, α-helices and *β*-sheet are shown as serpentine and arrow while the rest of the molecule represented as a *rope*

organized in 26 α–helices and 7 short *β*-sheets. *β*-strands (*β*-3–*β*-7), α–helices α-1 to α-5, α-14 to α-19 and α-22 to α-26 built most of the part of subdomain I while α-6 to α-13, two short *β*-strands (*β*-1 and *β*-2) and the following chain segments built up most of the subdomain II. The helices α-16 and α-17 provides the active site side-chains involved in the coordination of the catalytic zinc ion (His466 and His470 of α-16) and in catalysis (Glu469 of α-16).

Model validation

The refined LdDCP model was subjected to a series of three tests for its internal consistency and reliability. The first test was to compare the residue backbone conformations in LdDCP model by the inspection of Psi/Phi Ramachandran plot obtained from PROCHECK analysis and compared with the preferred values obtained from the Protein Data Bank of EcDCP. Ramachandran plot for LDCP model has 93.9% residues in most favorable regions with the remaining 5.7% of residues fall in additional allowed regions, 0.0% in generously allowed regions, 0.3% residues (2 out of the 677) in disallowed regions and G- factors; dihedrals: 0.23, covalent: 0.48, overall: 0.34.

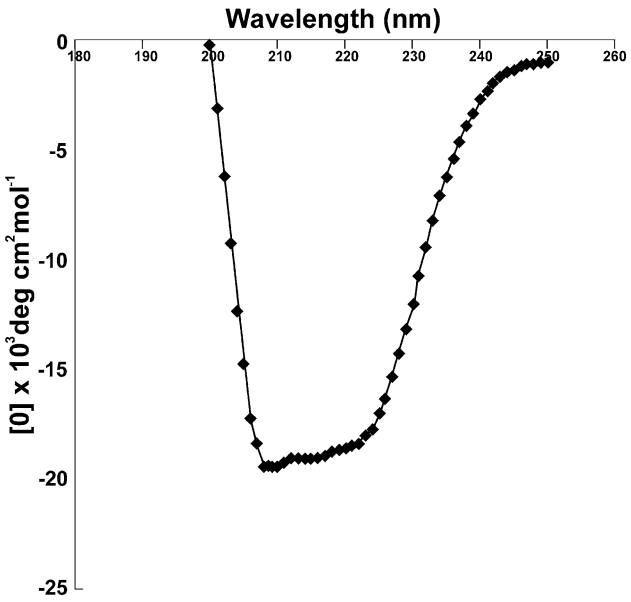

Fig. 5 Far-UV CD spectra of native recombinant LdDCP

Amino acid residues in disallowed conformations are located far from the putative active site of the protein. The spot distribution for the homology model of LdDCP was quite similar to the X-ray structure of EcDCP. Prosa II energy plot (second test) for LdDCP showed maximum residues to have negative interaction energy with the few residues displayed positive interaction energy (overall interaction energy −10.43) which is quite similar to the template EcDCP (−12.43). The third test used to evaluate the packing quality of refined structure (LdDCP) by the calculation of WHATIF quality control values (http://biotech.ebi.ac.uk:8400/). Table 1 depicts z-score for EcDCP (1.37) and LdDCP (−1.70). Overall Z-score of −5 or worse usually indicates poor packing. Since, there have been no residues in LdDCP model below this limit we concluded that the LdDCP model represents an acceptable packing quality. The back bone RMSD 0.2274, between the final minimized LdDCP homology model and the template EcDCP crystal structure further supports that the generated structure was reasonable good.

Docking studies of captopril

Docking studies not only provide an understanding of the binding mode of the ligands but also have employed to validate homology models [36]. The key characteristic of a good docking program is its ability to reproduce the experimental binding modes of ligands. To test this, a ligand is taken out of the X-ray structure of its protein-ligand complex and docked back into its binding site. The docked binding mode is then compared with the experimental binding mode, and a root-mean-square deviation

Table 1 WHATIF quality control values to determined the Pacing quality of refined LdDCP model and comparison with EcDCP crystal structure

Pacing quality	Backbone–backbone contacts	Backbone-side chain contacts	Sidechain-backbone contact	Side chain-side chain contacts	Z-score for all contacts
LdDCP	0.77	−3.35	−0.41	−3.21	−1.70
EcDCP	0.36	1.66	0.48	2.08	1.37

(RMSD) between the two is calculated; a prediction of a binding mode is considered successful if the RMSD is below a certain value (usually 2.0 Å). The reliability of the applied docking protocol was assessed by docking captopril into the active site of human ACE, taking as control (1UZF). The RMSD between the docked binding mode and the experimental binding mode of captopril in ACE was found within the cut-off limit (1.42 Å). The major interacting residues were determined to be His513, His353, Lys511, and Gln281. These residues are the same as reported earlier by X-ray structure analysis thus validating the docking protocol. FlexX dock score was calculated as −22.34 kJ/mole. Distance of Zinc ion from sulfur of docked captopril was 2.08 Å and from His383 & His387, it was 2.1 Å (Fig. 6a). The carboxyl group of captopril form two hydrogen bonds with Gln281 and one with Lys511, another carbonyl group form hydrogen bond with 2 histidine residues with N2 nitrogen of imidazole ring. The same docking protocol was then applied to dock captopril into the active sites of EcDCP and LdDCP. In case of EcDCP (1Y79), captopril interacts with His473, His469, Tyr614, Glu498 and Tyr607 residues. Carboxyl group of captopril forms two hydrogen bonds with Glu498, two hydrogen bonds with His473, one with Tyr614 and one with His469. FlexX dock score was calculated as −21.72 kJ/mole. Distance of Zinc ion from carboxyl group of docked captopril and from His473 to His469 of helix α 16 was 1.865 Å and 2.1 Å respectively (Fig. 6b). When captopril was docked into LdDCP, it binds to active site in same orientation as EcDCP and major interacting residues were Tyr604, Glu495 and His466. Carboxyl group of captopril forms only one hydrogen bond with Glu498, one with

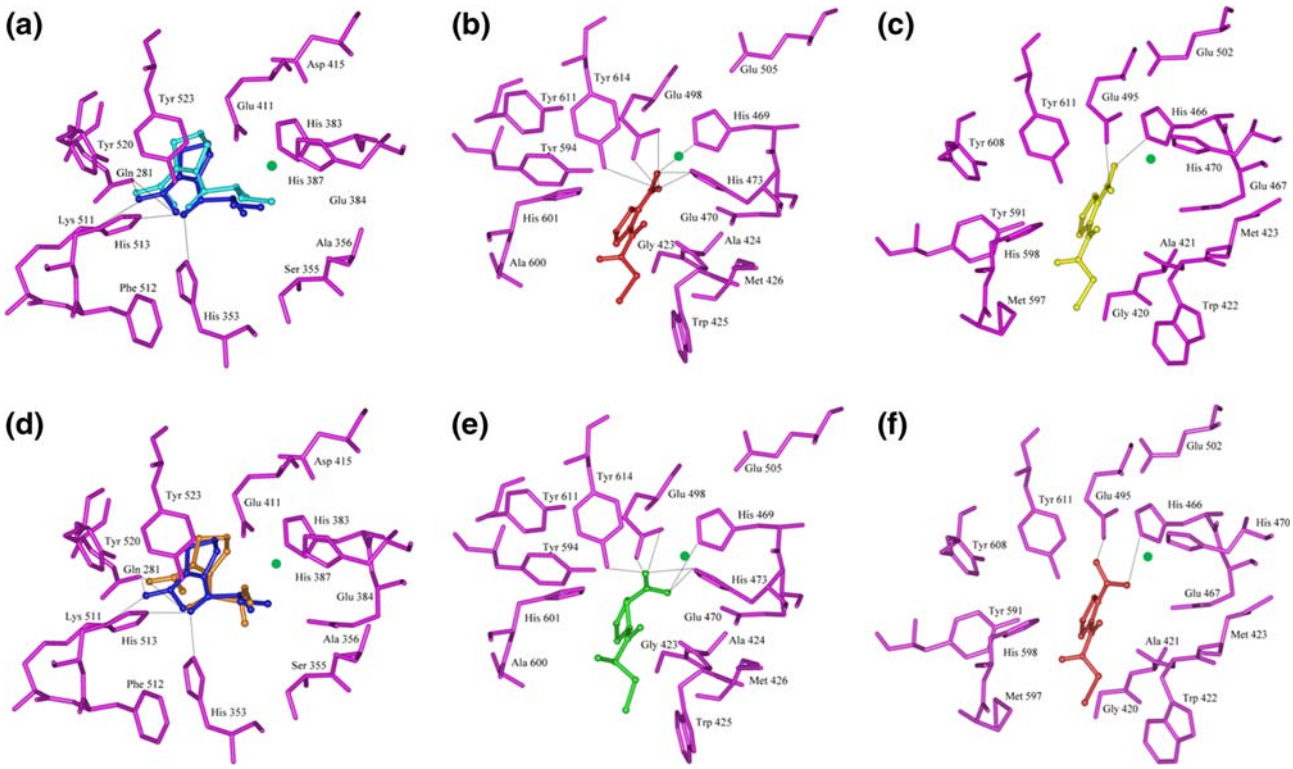

Fig. 6 Binding mode of captopril docked into the active site of ACE, EDCP and LdDCP **a** Crystal structure captopril (*Blue*) and docked captopril (*cyan*) in the active site of ACE using FlexX **b** Captopril (*red*) was docked in the active site of EcDCP using FlexX **c** Captopril (*yellow*) was docked in the active site of LdDCP using FlexX. Zinc ion is shown as *green color*. **d** Crystal structure captopril (*blue*) and docked captopril (*orange*) in the active site of ACE using LigandFit **e** Captopril (*green*) was docked in the active site of EcDCP using LigandFit **f** Captopril (*red*) was docked in the active site of LdDCP using LigandFit

Table 2 Ki values of captopril with htACE, EcDCP & LdDCP along with their corresponding docking score (FlexX & LigandFit) and MM-PBSA residue interaction energy

	Ki (nM)	FlexX dockscore (kJ/mol)	LigandFit dockscore	MM-PBSA residue interaction energy (kcal/mol)
htACE[a]	14	−22.34	41.512	−95.09
EcDCP[b]	NR	−21.72	40.055	−56.92
LdDCP	35.8	−21.01	39.648	−17.43

NR: not reported

[a] Deddish et al. 1996

[b] *E. coli* DCP exhibited a comparable exquisite sensitivity to captopril as human ACE [34]

Tyr604 and one with His466 (Try604 is not shown to get clarity in docking figure). FlexX dock score was calculated as −21.01 kJ/mole. Distance of Zinc ion from sulfur of docked captopril was 1.94 Å and from His466 is 2.1 Å (Fig. 6c). To have a comparative analysis and validation of our docking results we checked the bound conformation derived from FlexX docking using another molecular docking software, LigandFit. The bound conformations of captopril with ACE, EcDCP and LdDCP derived from LigandFit docking are represented in Fig. 6d, e and f, respectively. The top ranked docked poses for captopril to ACE, EcDCP and LdDCP active site from LigandFit docking were almost similar to the FlexX results. LigandFit dockscores for the top ranked docking solution of ACE, EcDCP and LdDCP were 41.512, 40.055 and 39.648 respectively. The Dock Score derived from LigandFit docking was also in correlation with the biological activity of captopril against ACE, EcDCP and LdDCP (Table 2).

These docking studies revealed that captopril binding mode was different in all three proteins. Although inhibitor placed itself in same orientation in both EcDCP and LdDCP but number of hydrogen bonds with interacting residues were only three in LdDCP as compared to six in EcDCP. Also, His 473 interaction with captopril observed in EcDCP was absent in LdDCP. Probably this interaction is responsible for better binding of captopril to EcDCP thus for higher inhibition [34]. In case of ACE, captopril fits itself in entirely different orientation because of difference in shape and conformation of active site. The interacting residues with captopril in ACE were also found different from EcDCP or LdDCP. These relative differences in the active site should undoubtedly affect the steric and electrostatic interactions with inhibitors. Thus the model can explain variations in Ki values of captopril which in return related to binding affinity of inhibitor. On comparing the amino acid residues of active site (6.5 Å) around the docked captopril of htACE with LdDCP and EcDCP revealed eight residues that were highly conserved in all three enzymes (Ala421, His598, Glu467, His466, Tyr608, Tyr611, His470 and Glu495) as shown in Fig. 7. Except

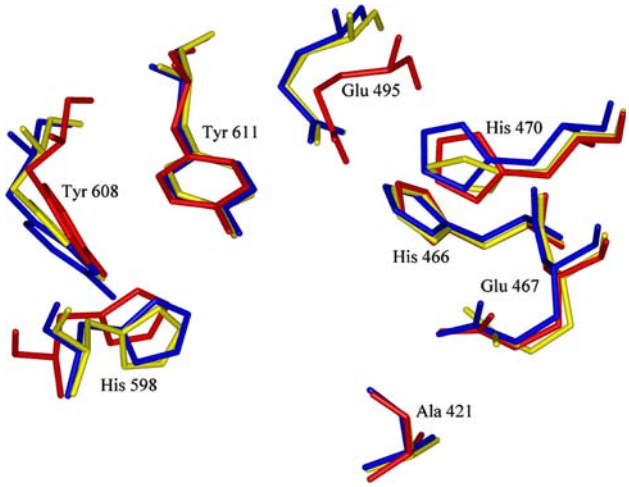

Fig. 7 Superimposition of conserved active site amino acid residues of LdDCP (*yellow*) onto the EcDCP (*blue*) and human ACE (*red*). LdDCP residues are labeled

two (Met597 and Val547 residues in EcDCP, replaced by Ala600 and Leu550, respectively, in LdDCP), all other residues were same in LdDCP and EcDCP. While in the case of ACE, remaining residues were entirely different. These changes in the active sites of EcDCP, LdDCP and ACE presumably play a significant role in the observed differences in substrate specificity and inhibitor binding profile for these homologue enzymes.

MM/PBSA interaction energy

The experimental activity and docking studies are successful to some extent to explain the modest selectivity of captopril for LdDCP and EcDCP but excellent selectivity for ACE. However, to better understand the mechanisms of the selectivity, the MM-PBSA residue interaction energy of bound conformation of captopril derived from docking using Discovery Studio Package was calculated. The calculated total interaction energies of captopril with ACE, EcDCP, and LdDCP were −95.09, −56.92, and −17.43 kcal/mol,

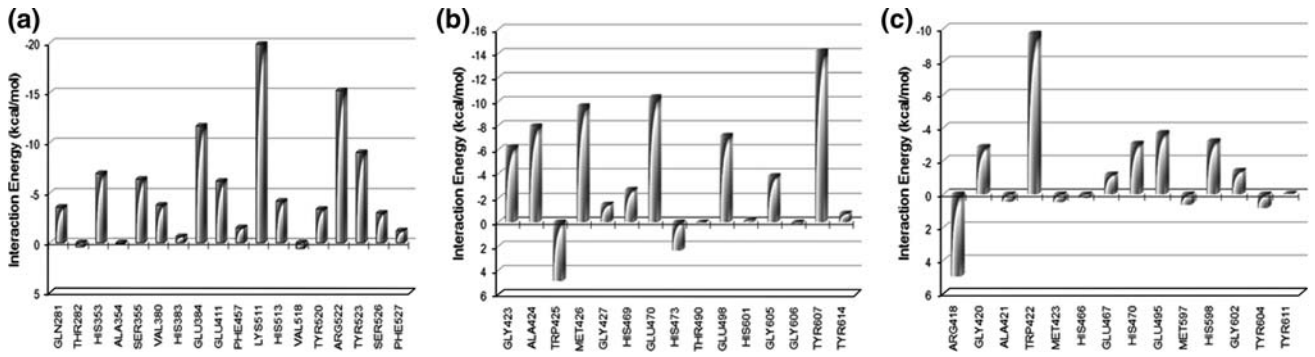

Fig. 8 Captopril-residue interaction spectrums of **a** Captopril-ACE **b** Captopril-EcDCP and **c** Captopril-LdDCP

respectively, which were consistent with the experimental and docking results (Table 2). In order to get an insight of contribution of each residue to the total interaction energy, energy decomposition analysis was carried out (Fig. 8), which gives a direct view about the selectivity of captopril. The active site of ACE includes amino acid residues Gln281, Thr282, His353, Ala 354, Ser355, Val380, His383, Glu384, Glu411, Phe457, Lys511, His513, Val518, Tyr520, Arg522, Tyr523, Ser526 and Phe527. The residues similar to the corresponding EcDCP and LdDCP active site are Ala354, His383, His387, Glu411, His513, Tyr520 and Tyr523. The two significant contributors to the interaction energy between captopril and ACE were Lys511 and Arg522 with interaction energy of −19.86 and −15.20 kcal/mol, respectively. These amino acid residues are absent in the active site EcDCP and LdDCP and hence accounts for greater selectivity to ACE than EcDCP and LdDCP. However, it does not escape from the high homology between the active sites of three proteins (Fig.7). The moderate selectivity of EcDCP towards captopril is because of the contributions from Glu470 with interaction energy of −10.36 kcal/mol compared to interaction energy of −11.64 kcal/mol for Glu384 of ACE (Fig. 8b). As there are almost no contribution from corresponding Glu467 in LdDCP there is very less selectivity towards LdDCP. The significant contribution to interaction energy between captopril and LdDCP are from Trp522, His470 and Glu 495 (Fig. 8c). Therefore, in order to design more selective inhibitors towards LdDCP, an identification of some scaffolds/some functional groups are required that better interact with Glu467, His470, Glu495 via hydrogen bonding and with Trp522 via some hydrophobic interactions. High polarity and large volume may be helpful to improve the selectivity considering the high polarity of the binding site.

Molecular electrostatic potential

MEP is an electrical effect of electrons and nuclei of a molecule in its vicinity [23]. In case of a ligand–protein interaction, at the active site, the ligand experiences a unique environment in terms of electrostatic, steric and hydrophobic properties. Therefore, MEP affects the strength of interaction of the ligand with the receptor protein and is evolutionary selected by a protein to perform a specific function [37]. The electrostatic potential on a molecular surface can be used to visually compare two molecules, guiding docking studies and identifying sites that interact with ligands. A comparison of molecular electrostatic potential (MEP)s of ACE, EcDCP and LdDCP was made as a first step toward the design of specific inhibitors for LdDCP. As expected, the electrostatic potential as well as shapes of active site cavities are different for all the three proteins (Fig. 9). Although LdDCP and EcDCP appear to have a similar shape, but the cavity groove of LdDCP is more electronegative compared to EcDCP. The shape and electrostatic potential covering the active site residues in ACE was entirely different (mostly electropositive residues are predominant in active site).These differences further confirm differential recognition and binding pattern of captopril with ACE, EcDCP and LdDCP.

Conclusion

The major obstacle in application based drug design is the lack of structural data for putative/validated targets. This is where homology or comparative modeling comes to rescue, by which it is easier to predict the structure of the target protein with the help of structurally resolved template protein. Present study demonstrate that Leishaminal DCP significantly differ from bacterial DCP and human ACE in kinetic properties (Km and Ki) due to several minor but potentially important structural differences at the active site of these three functionally similar enzymes. These differences can be exploited in the early design and development of selective LdDCP inhibitors. Efforts are underway in our laboratory to identify inhibitors of LdDCP for their antileishmanial potential using this model by in silico docking of databases of institutional chemical

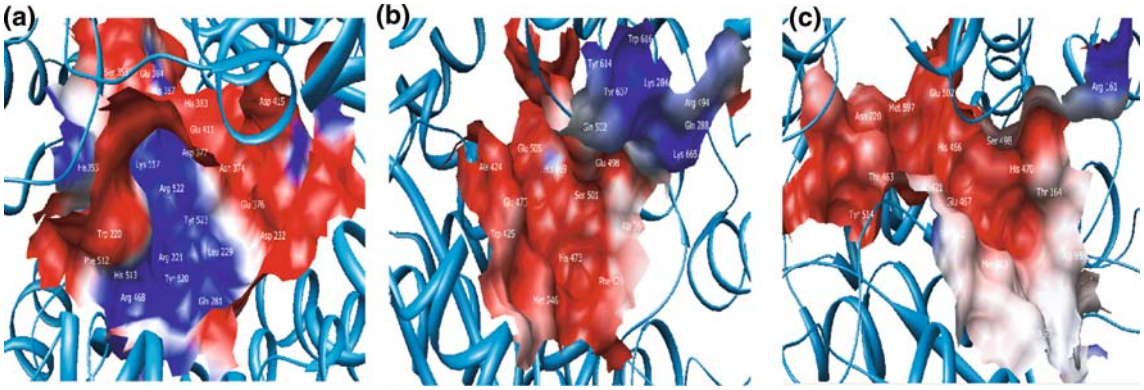

Fig. 9 The molecular electrostatic potential (MEP) displayed for active sites of **a** ACE **b** EcDCP and **c** LdDCP. The deep blue color indicates the highest positive potential whereas the most negative potential is seen as a *deep red color*

compounds. Thus, the present structure indeed prospects the possibility of using structural based design to develop completely novel DCP inhibitor that selectively inhibit LdDCP without affecting ACE and might thus represents an important step towards the establishment of antileishmanial chemotherapy.

Acknowledgments This manuscript carries CDRI communication number 7523. The work is supported by grant from Council of Scientific and Industrial Research (CSIR) funded network project NPW0038 'Identification and validation of drug targets for selected pathogen' and CSIR for financial support to M.S.B and Ashutosh Kumar.

References

1. Handman E (2001) Leishmaniasis: current status of vaccine development. Clin Microbio Rev 14:229
2. Ashford RW, Desjeux P, Deraadt P (1992) Estimation of population at risk of infection and number of cases of Leishmaniasis. Parasitol Today 8:104
3. Molyneux D, Killick-Kendrick R (1987) Morphology, ultrastructure and lifecycles. In: The Leishmaniasis in biology and medicine, vol 1, pp 121
4. Guerin PJ, Olliaro P, Sundar S, Boelaert M, Croft SL, Deseux P, Wasunna MK, Bryceson AD (2002) Visceral leishmaniasis: current status of control, diagnosis and treatment and a proposed research and development agenda. Lancet Infect Dis 2:494
5. Rijal S, Chappuis F, Singh R, Bovier PA, Achrya A, Karki BM, Das ML, Deseux P, Loutan L, Koirala S (2003) Treatment of visceral leishmaniasis in south eastern Nepal: decreasing efficacy of sodium stibogluconate and need for policy to limit further decline. Trans R Soc Trop Med Hyg 97:350
6. Goyal N, Duncan R, Selvapandiyan A, Debrabant A, Baig MS, Nakhasi HL (2006) Cloning and characterization of angiotensin converting enzyme related dipeptidylcarboxypeptidase from *Leishmania donovani*. Mol Biochem Parasitol 145:147
7. Fiser A (2004) Protein structure modeling in the proteomics era. Expert Rev Proteomics 1:97
8. Lesk AM, Chothia C (1980) How different amino acid sequences determine similar protein structures: the structure and evolutionary dynamics of the globins. J Mol Biol 136:225
9. Chothia C, Lesk AM (1986) The relation between the divergence of sequence and structure in proteins. EMBO J 5:823
10. Comellas-Bigler M, Lang R, Bode W, Maskos K (2005) Crystal structure of *E. coli* dipeptidylcarboxypeptidase DCP:future indication of a ligand dependent hinge movement mechanism. J Mol Biol 349:99
11. Lammeli UK (1970) Cleavage of structrural proteins during the assembly of the head of bacteriphage T4. Nature 227:80
12. Cushman DW, Cheung HS (1971) Spectrophotometric assay for angiotensin converting enzyme. Biochem Pharmacol 20:1637
13. Bradford MM (1976) A rapid and sensitive method for the quantitation of microgram quantities of protein utilizing the principle of protein dye binding. Anal Biochem 72:248
14. Sali A, Blundell TL (1993) Comparative protein modelling by satisfaction of spatial restraints. J Mol Biol 234:779
15. Peng Y, Keenan SM, Welsh WJ (2005) Structural model of *Plasmodium* CDK, Pfmrk, a novel target for malaria chemotherapy. J Mol Graph Mod 24:72
16. Gellert A, Salanki K, NaraySzabo G (2006) Homology modeling and protein structure based functional analysis of cucumovirus coat proteins. J Mol Graph Mod 24:319
17. Heo J, Vaidehi N, Wendel William A (2007) Prediction of 3D structure of rat Mrg A G protein coupled receptor and identification of its binding site. J Mol Graph Mod 26:800
18. Laskowaski RA, McArther MW, Moss DS, Thornton JM (1993) PROCHECK: a program to check sterio-chemical quality of a protein structures. J Appl Crystalogr 26:283
19. Hooft RWW, Vriend G, Sander C, Abola EE (1996) Errors in protein structures. Nature 381:272
20. Hooft RWW, Sander C, Vriend G (1996) Verification of protein structures: side chain planarity. J Appl Crystallog 29:714
21. Natesh R, Schwager SL, Sturrock ED, Acharya KR (2003) Crystal structure of the human angiotensin-converting enzyme-lisinopril complex. Nature 421:551
22. Nicholls A, Sharp KA, Honig B (1991) Protein Folding and Association: Insights from the Interfacial and Thermodynamic Properties of Hydrocarbons. Proteins Stuc Func Genet 11:281
23. Politzer P, Laurence PR, Jayasuriya K (1985) Molecular electrostatic potentials: an effective tool for the elucidation of biochemical phenomena. Environ Health Perspect 61:191
24. Pettersen EF, Goddard TD, Huang CC, Couch GS, Greenblatt DM, Meng EC, Ferrin TE (2004) UCSF Chimera—A Visualization System for Exploratory Research and Analysis. J Comput Chem 25:1605
25. Mottram JC, Coombs GH, Alexander J (2004) Cysteine peptidase as virulence factors of *Leishmania*. Curr Opin Microbiol 7:375
26. Yao C, Donelson JE, Wilson ME (2003) The major surface protease (MSP or GP63) of *Leishmania* species: biosynthesis, regulation of expression and function. Mol Biochem Parasitol 132:1

27. Andrade Ribeirode AS, Santero MM, de Melo NN, Mares-Guia M (1998) *Leishmania (Leishmania) amazonensis*: purification and enzymatic characterization of soluble serein oligopeptidase. Exp Parasitol 89:153
28. Morty RE, Morehead J (2002) Cloning and characterization of leucylaminopeptidase from three pathogenic *Leishmania* species. J Biol Chem 277:26057
29. Yaron A, Mlynar D, Berger A (1972) A dipeptidocarboxypeptidase from *E. coli*. Biochem Biophys Res Commun 47:897
30. Soffer RL, Das M, Caldwell PR, Seegal BC, Hsu KC (1976) Biological and biochemical properties of angiotensin converting enzyme. Agents Actions 6:534
31. Lanzillo JJ, Dasarathy Y, Stevens J, Bardin CW, Fanburg BL (1985) Human testicular angiotensin-converting enzyme is a mixture of two molecular weight forms, Only one is similar to the seminal plasma enzyme. Biochem Biophys Res Commun 128:457
32. Henrich B, Becker S, Schroeder U, Plapp R (1993) dcp Gene of *Escherichia coli*: Cloning, sequencing, transcript mapping and characterization of the gene product. J Bacteriol 175:7290
33. Deddish PA, Wang LX, Jackman HL, Michel B, Wang J, Skidgel RA, Erdös EG (1996) J Pharmacol Exp Ther 279:1582
34. Deutch CE, Soffer RL (1978) *Escherichia coli* mutant defective in dipeptidyl carboxypeptidase. Pro Natl Acad Sci USA 75:5998
35. Junot C, Gonzales MF, Ezan E, Cotton J, Vazeux G, Michaud A, Azizi M, Vassiliou S, Yiotakis A, Corvol P, Dive V (2001) RXP 407, a selective inhibitor of the N-domain of angiotensin I-converting enzyme, blocks in vivo the degradation of hemoregulatory peptide acetyl-Ser-Asp-Lys-Pro with no effect on angiotensin I hydrolysis. J Pharmacol Exp Ther 297:606
36. Singh N, Chevé G, Avery MA, McCurdy CR (2006) Comparative protein modeling of 1-deoxy-D-xylulose-5-phosphate reductoisomerase enzyme from *Plasmodium falciparum*: a potential target for antimalarial drug discovery. J Chem Inf Model 46:1360
37. Sinha N, Smith-Gill SJ (2002) Electrostatics in protein binding and function. Curr Protein Pept Sci 3:601